Construction of a Picosecond Time-Resolved IR Dip Spectrometer for Studying Structures and Dynamics of Solvated Clusters

Makoto Sakai, Tadashi Ueda,[†] Takaya Yamanaka,[†] and Masaaki Fujii*,[#]

Institute for Molecular Science and The Graduate University for Advanced Studies, Myodaiji, Okazaki 444-8585

†Laser Research Center for Molecular Science, Institute for Molecular Science, Myodaiji, Okazaki 444-8585

(Received May 15, 2002)

We have constructed a picosecond time-resolved IR dip spectrometer having a frequency resolution of < 20 cm^{-1} and an instrument response time of 25 ps. In this system, the second harmonic of the idler wave from the OPA pumped at 800 nm and the remaining light from a regenerative amplifier (< 2.5 mJ/pulse) were differentially mixed in a KTA crystal to generate tunable high-power IR light (2750–4000 cm^{-1}; > 60 μJ). The picosecond time-resolved IR dip spectra of phenol–$(H_2O)_1$ and carbazole–$(H_2O)_1$ are presented to demonstrate the capability of the constructed system. The spectral changes show clear vibrational structures of not only S_0, but also S_1 in the 2800–3800 cm^{-1} energy region. The system performance is also discussed.

A solvated cluster has historically been considered to be a part of a condensed-phase, and much research had been conducted over the years. Recently, hydrogen-bond networks in solvated clusters in the gas phase have been extensively investigated based on the IR spectrum, which has become available owing to the various nanosecond IR-UV double resonant spectroscopies that use a strong and tunable infrared pulsed laser.[1–6] For a cluster in the ground state, the typical method is IR dip spectroscopy. In principle, this method can measure the IR transition even in the S_1 state where various photochemistry events occur. Nevertheless, only a few examples[7–10] have been reported concerning the IR spectroscopy of S_1 clusters. Furthermore, IR-UV double-resonance spectroscopy has rarely been applied to photochemically activated clusters, except for a system in which the reaction product has a long lifetime, such as hydrogen-transfer in phenol/ammonia clusters.[11,12] The obvious problem is a lack of time resolution in IR and UV lasers, because the lifetime of S_1 is of the nanosecond order as a general case. From this motivation, a new IR-UV double resonant spectroscopic technique is required that permits a time resolution of less than a few picoseconds. The most crucial factor in designing a picosecond time-resolved IR dip spectrometer is choosing the picosecond pulsed IR light source. An IR dip measurement requires that the IR light has high-energy power to produce a substantial number of vibrational excitations; moreover, the IR frequency must be scanned continuously in the 2800–3800 cm^{-1} mid-IR region. If the generation of the mid-IR light satisfies our requirements as mentioned above, picosecond time-resolved IR dip spectroscopy will become a powerful tool for monitoring the structure of short-lived S_1 clusters, as well as the ultrafast dynamics of photochemically activated clusters in the gas phase.

In order to utilize this method for studying the structure and dynamics of ultrafast reactive molecules in condensed phases, various approaches have been carried out to generate picosecond mid-IR light up until the present time.[13–26] The OPG, OPA, and DFG techniques, based on mode-locked lasers, such as Nd:YAG, Nd:glass, and Ti:sapphire, were widely applied to generate mid-IR pulses, except for free-electron lasers. Especially, Dlott's group obtained powerful and tunable mid-IR pulses of 40–50 μJ energy by using the OPA technique based on a regenerative amplified Ti:sapphire laser with a Nd:YAG seed, and succeeded in applying ultrafast infrared-Raman studies of the vibrational energy redistribution in polyatomic liquids by using IR light for the pumping source.[27–29] In their system, mid-IR pulses have sufficient power to produce a substantial number of vibrational excitations. On the other hand, the scanning of IR light was too difficult because it was tuned over ~1000 cm^{-1} by tuning the wavelength of a regenerative amplified Ti:sapphire laser, which was the main part of their system. Therefore, we adopted a new design in which the second harmonic of the idler wave from the OPA pumped at 800 nm and the remaining light from a regenerative amplifier are differentially mixed in a potassium titanyl arsenate (KTA) crystal. In this method, the IR light can be scanned only by a computer program control of the rotational crystal stage. In the experimental section, the result of mid-IR generation is described in detail.

In this present paper, we report on the construction of a picosecond time-resolved IR dip spectrometer with high-power mid-IR generation; also the picosecond time-resolved IR dip spectra of phenol–$(H_2O)_1$ and carbazole–$(H_2O)_1$ clusters are presented to demonstrate the use of picosecond time-resolved fluorescence detected (TRFD) IR dip spectroscopy. The IR transition in the S_1 state was clearly measured in both solvated clusters. Based on an analysis of their spectra, the system performance is also discussed in detail.

[#] Laser Research Center for Molecular Science, Institute for Molecular Science

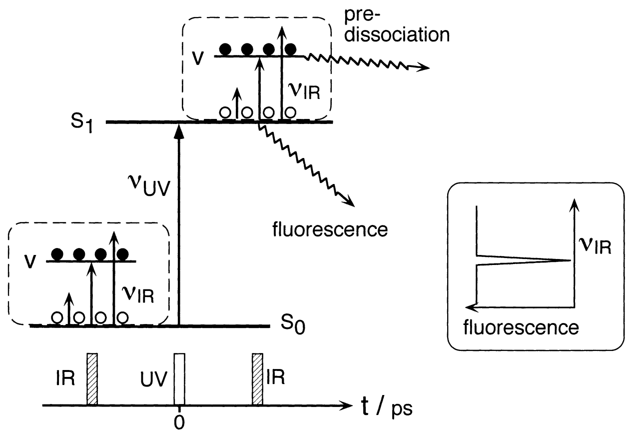

Fig. 1. Principle of picosecond time-resolved fluorescence detected IR dip spectroscopy.

Experimental

1. Principle of Picosecond Time-Resolved Fluorescence Detected IR Dip Spectroscopy. Figure 1 shows the principle of picosecond time-resolved fluorescence detected (TRFD) IR dip spectroscopy for measuring the IR transition in the S_1 state. This method is based on nanosecond IR dip spectroscopy, except for using picosecond IR and UV light sources. Briefly, a molecular cluster is excited to S_1 by a picosecond UV laser. After an appropriate delay, the S_1 cluster is further excited by a picosecond IR laser that is scanned over the vibrational region in S_1. When the IR frequency is resonant to the vibrational level in S_1, the fluorescence intensity decreases because of a lower fluorescence quantum yield in the higher vibrational state. Thus, the IR spectrum in S_1 can be measured as a depletion of the fluorescence intensity. When the delay time is minus, i.e. IR irradiates before UV, the IR depletion corresponds to the IR transition in S_0 (see Fig. 1).

2. Laser Setup. A schematic drawing of the picosecond laser system is given in Fig. 2. The laser system is based on a cw mode-locked Ti:sapphire laser (Spectra Physics, Tsunami) with a pulse duration of 130 fs, pumped by a 5 W diode laser (Spectra Physics, Millennia Vs). The output pulses (550 mW; 82 MHz) from the oscillator are amplified at a repetition rate of 10 Hz in a regenerative Ti:sapphire amplifier (Quanta Ray, TSA-10) pumped by the frequency-doubled output of a Nd:YAG laser (Quanta Ray, GCR 130). By masking the grating in a regenerative Ti:sapphire amplifier, the time duration and energy of the amplified output pulses are 2–3 ps and > 5.5 mJ/pulse at 800 nm. The output is divided into two beams. One beam (1 mJ/pulse) is used to pump a traveling-wave optical parametric amplifier (OPA) system (Light conversion, TOPAS 400) after frequency doubling in BBO, and to provide the tunable UV light (250–390 nm; > 15 μJ) by the second harmonics of the signal (or idler) wave from the OPA. The other (< 4.5 mJ/pulse) is further split into two beams, one of which is introduced into another OPA system (Light conversion, TOPAS 800). The second harmonic of the idler wave from the OPA and the remaining fundamental light (< 2.5 mJ/pulse) were differentially mixed in a KTA crystal to generate tunable IR light (2750–4000 cm^{-1}; > 60 μJ). We employed this new design of the IR generation method to obtain high power. The tunable IR output power as a function of the wavenumber (cm^{-1}) is shown in Fig. 3. It shows that the IR output power is more than equal to that of the system of Dlott's group; furthermore, the scanning is also possible in this region. This new IR generation method is thus quite useful, and the system is enough to carry out IR dip spectroscopy. The laser auto-correlation time of the UV or IR light and the cross-correlation time between them are typically around 2–3 ps, which depends on the wavelength. The line width of UV light was determined to be about 10 cm^{-1} by measuring the S_1 origin of several samples in the gas phase. The line width of IR light is described later.

3. Experimental Setup. Both the IR laser and the UV laser from the picosecond laser system were coaxially introduced into a vacuum chamber (Toyama/Hakuto) and crossed a supersonic jet. The sample was irradiated with the IR laser before/after the UV laser at several delay times. The delay time between the IR laser and the UV laser varied by an optical delay system (Sigma, LTS-400X; 5 μm/step) which ranged from −500 ps to 1.5 ns. The fluorescence from the sample was collected by a lens and detected by a photomultiplier (Hamamatsu, 1P28) through filters (Toshiba, UV-29 or UV-35/Corning, 7-54). The signal was amplified by a preamplifier (EG&G PARC, 5113) and was integrated by a digital boxcar (EG&G PARC, 4420/4422). The integrated signal was recorded by a personal computer as a function of the IR laser frequency.

Phenol vapor at 293 K (or carbazole vapor at 398 K) was seeded in He gas at 3 atm, which contained water vapor at 263 K. The mixture was then expanded into the vacuum chamber through a pulsed nozzle operated at 10 Hz. Samples were purchased from Tokyo Kasei and were used after purification.

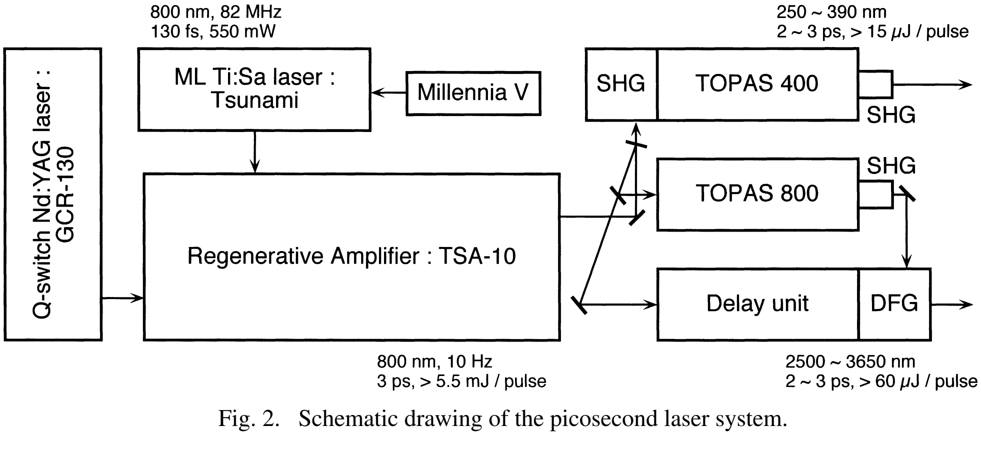

Fig. 2. Schematic drawing of the picosecond laser system.

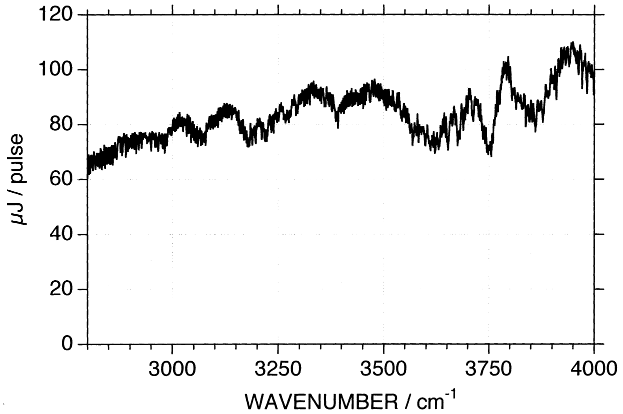

Fig. 3. Tunable IR output power as a function of the wavenumber (cm^{-1}).

Results and Discussion

1. Phenol–$(H_2O)_1$ Cluster. In order to check the frequency resolution and the instrument response time of our constructed system, we measured the picosecond TRFD IR dip spectra of a phenol–$(H_2O)_1$ cluster. A phenol–$(H_2O)_1$ cluster is a rare example of the case in which the IR dip spectrum has been measured not only in S_0, but also in S_1, because of its long lifetime (6 ns in S_1). In a previous report,[8] the phenolic OH stretching vibrations (ν_{OH}) in S_0 and S_1 were assigned to bands at 3524 cm^{-1} and 3388 cm^{-1}, respectively. The results of picosecond TRFD IR dip measurements are shown in Fig. 4 (a). These IR spectra were measured at various delay times before/after the irradiation of UV light (35994 cm^{-1}). The excitation schemes of fluorescence detected IR dip spectroscopy for the S_0 state and for the S_1 state are different as regards the timing between the IR laser and the UV laser. When the IR laser was irradiated before the UV laser, the IR spectrum of the cluster in S_0 was obtained by scanning the IR frequency. When the IR laser was irradiated after the UV laser, the IR dip spectrum of the S_1 clusters was obtained.

Figure 4 (a) shows that at a -100 ps delay time the phenol–$(H_2O)_1$ cluster exhibited an IR absorption band at 3524 cm^{-1} that is attributable to the phenolic ν_{OH} in S_0.[8] With time, the 3524 cm^{-1} band in S_0 rapidly decreased in intensity; on the other hand, a new band at 3388 cm^{-1} that is attributable to the phenolic ν_{OH} in S_1[8] was observed clearly. Here, the bandwidths were measured to be ~19.9 cm^{-1} at the 3524 cm^{-1} band and ~24.1 cm^{-1} at the 3388 cm^{-1} band, respectively. The bandwidths of ν_{OH} of phenol–$(H_2O)_1$ in S_0 and S_1 were reported to be around ~5 cm^{-1}.[8] Thus, from the observed bandwidth, the frequency resolution of IR light was estimated to be < 20 cm^{-1}. The time-evolution of the peak intensity of the 3524 cm^{-1} band and the 3388 cm^{-1} band are also shown in Fig. 4 (b). The decay and rise traces fitted to the observed profiles by a Gaussian function are also indicated by the solid curve. The decay and rise times, that is the instrument response times, were measured to be ~28.1 ps in the 3524 cm^{-1} band and ~20.7 ps in the 3388 cm^{-1} band, respectively. Therefore, the instrument response time was estimated to be about 25 ps.

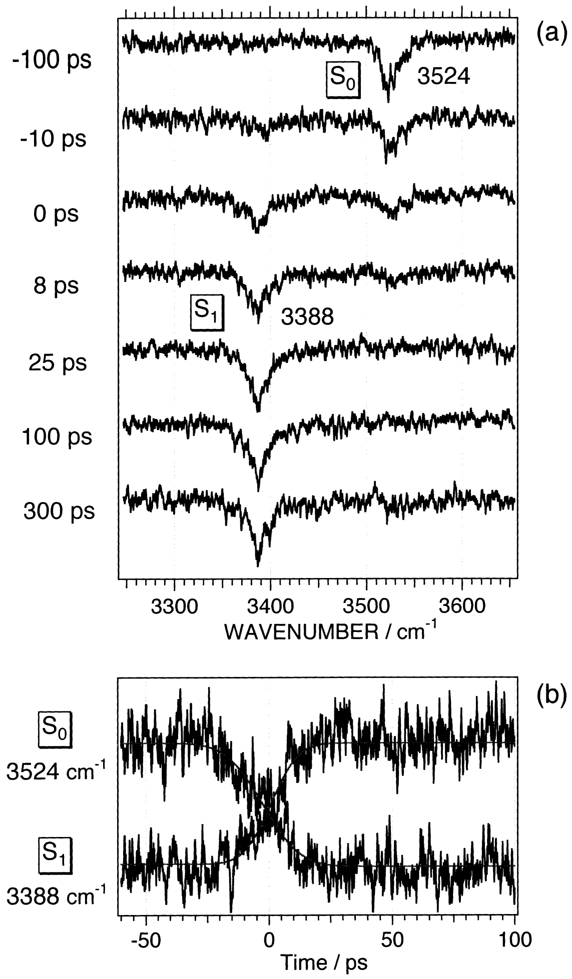

Fig. 4. (a) Picosecond TRFD IR dip spectra of a phenol–$(H_2O)_1$ cluster measured at various delay times before/after UV pumping (35994 cm^{-1}). The bandwidths were measured as ~19.9 cm^{-1} at 3524 cm^{-1} band and ~24.1 cm^{-1} at 3388 cm^{-1} band, respectively. (b) The time-evolution of the peak intensity of the 3524 cm^{-1} band and the 3388 cm^{-1} band. The instrument response traces fitted to the observed profiles by a Gaussian function are also shown by the solid curve. The instrument response time were estimated to be ~28.1 ps at the 3524 cm^{-1} band and ~20.7 ps at the 3388 cm^{-1} band, respectively.

From the time-resolved spectra of phenol–$(H_2O)_1$, the frequency resolution of IR light was estimated to be < 20 cm^{-1}, and the instrument response time was about 25 ps. It is noted that the instrument response time (25 ps) deteriorated significantly from the laser cross-correlation (around 2–3 ps). This is because the IR and UV lasers were counterpropagated to free-jet expansion in a vacuum chamber. To obtain higher time-resolution, the IR and UV lasers should be introduced into a vacuum chamber in a colinear setting from the same direction, or the free-jet expansion should be skimmed by a skimmer. However, such deterioration was only less than 20 ps. This was because both the IR and UV lasers were focused on a supersonic free jet by using $f = 250$ mm lenses, and, at that time, the optical length given the IR dip signal became shorter than about 5 mm. Therefore, we could get a good performance without both a colinear setting and a skimmer. Considering the great

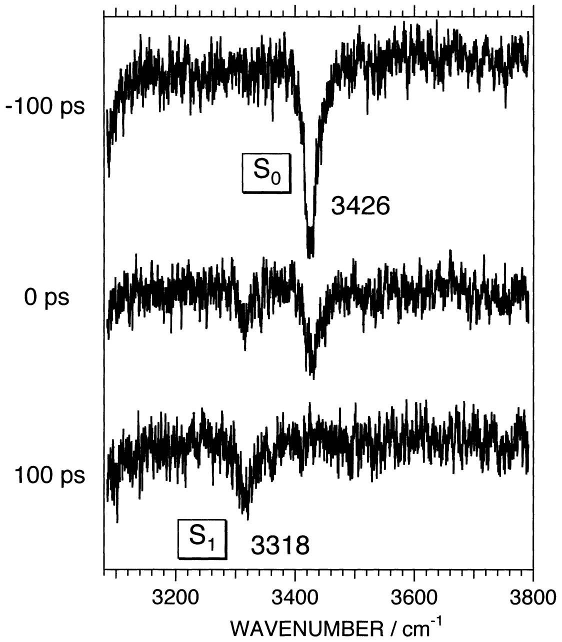

Fig. 5. Picosecond TRFD IR dip spectra of a carbazole–$(H_2O)_1$ cluster measured at various delay times before/after UV pumping (30317 cm^{-1}). The bandwidths were estimated to be ~22.7 cm^{-1} at 3426 cm^{-1} band and ~26.7 cm^{-1} at 3318 cm^{-1} band, respectively.

advantage of easily obtaining an IR dip signal, our experimental setup is acceptable for our purpose.

2. Carbazole–$(H_2O)_1$ Cluster. It is shown in the previous section that the picosecond TRFD IR dip spectroscopy can measure the vibrational transition with < 20 cm^{-1} of energy-resolution and 25 ps of time-resolution. To clarify the characteristics of picosecond TRFD IR dip spectroscopy, it was applied to a carbazole–$(H_2O)_1$ cluster. It is known that carbazole indicates a clear solvent dependence in photochemical reactions after two-photon excitation.[30–32] In a non-polar solution, it has been shown that the primary product is a neutral carbazyl radical (9*H*-carbazol-9-yl radical). On the other hand, in a polar solution, the main product is changed to a cation radical. In order to understand the mechanism of the photochemical reactions after two-photon excitation, it is of primary importance to reveal the structures and dynamics of photolytically generated transient molecular species, including excited electronic states such as the S_1 state and the cation state (D_0). Nevertheless, the structures of these species are not well-known. In order to clarify this interesting problem, we measured the picosecond time-resolved IR dip spectra of the carbazole–$(H_2O)_1$ cluster in the beginning.

Figure 5 shows the picosecond TRFD IR dip spectra of a carbazole–$(H_2O)_1$ cluster by fixing the UV laser to the S_1 origin (30317 cm^{-1}).[33] It can be seen in Fig. 5 that at -100 ps delay time the carbazole–$(H_2O)_1$ cluster exhibits an IR absorption band at 3426 cm^{-1} that is attributable to the NH stretching vibration of carbazole (ν_{NH}) in S_0. This vibrational frequency coincided with our previous result based on nanosecond IR dip spectroscopy.[34] On the other hand, at 100 ps delay time the 3426 cm^{-1} band in S_0 goes out of sight and the band at 3318 cm^{-1} that is attributable to ν_{NH} in S_1 was observed weakly. Those bandwidths were measured as ~22.7 cm^{-1} at the 3426 cm^{-1} band and ~26.7 cm^{-1} at the 3318 cm^{-1} band, respectively. It is noticed that the 3318 cm^{-1} band in S_1 remarkably decreases in intensity compared to the 3426 cm^{-1} band in S_0.

When the IR frequency is resonant to a certain vibrational transition in S_1, the cluster is vibrationally excited in S_1. In general, the fluorescence quantum yield from the higher vibronic band in S_1 is much lower than that from the zero-point level of the S_1 clusters because of acceleration of the non-radiative process. Thus, a strong IR dip signal was obtained [see Fig. 4 (a)]. In the case of carbazole–$(H_2O)_1$, on the other hand, the IR dip signal of the S_1 cluster was obtained weakly (see Figure 5). This means that the total fluorescence intensity does not vary much between before and after IR irradiation. It suggests that the fluorescence quantum yield from the S_1 vibronic level is about the same as that of the S_1 origin, or that a monomer generated after predissociation fluoresces strongly.[10] In future work, the fluorescence should be dispersed so as to separate the fluorescence due to the cluster from that from the monomer. However, we would like to emphasize that the IR transition in S_1 has been clearly detected by the picosecond laser system even under this condition. In fact, we could not observe this slight change when we carried out the same experiment using a nanosecond laser with about a 10 ns pulse width, which is comparable to the S_1 lifetime.

Here, it should be noted that vibrations of the water moiety were not observed in this system. With use of a nanosecond laser system, the IR dip spectrum of a carbazole–$(H_2O)_1$ cluster shows two bands at 3652 and 3748 cm^{-1} in the high-energy region.[34] They have been assigned to the symmetric and antisymmetric vibrations of the water moiety (ν_1 and ν_3), respectively. With use of a picosecond laser system, however, only the band of ν_{NH} was observed strongly, and two bands at 3652 and 3748 cm^{-1} disappeared, or were barely observed because the band intensity was close to the background noise. One of the reasons for this problem was that those oscillator strengths are much weaker than ν_{NH}. The other is that the bandwidths of ν_1 and ν_3 were narrower than the laser line width. That caused ineffective pumping. In order to improve this situation, the laser output needs to be improved regarding the energy resolution and power.

As stated above, our constructed picosecond system could not obtain weak, sharp bands, such as free OH stretching bands. On the other hand, the key vibrations to characterize the structures in solvated clusters were clearly observed, such as the hydrogen-bonded OH stretching mode and the NH stretching in Figs. 4 (a) and 5. They clearly show that the picosecond system has sufficient potential to investigate hydrogen-bond networks in photo-excited clusters.

The observed frequencies and bandwidth of ν_{NH} in S_0 and S_1 are compared in Table 1. The bandwidth was estimated by assuming that the IR light has a Gaussian distribution with a $<$ 20 cm^{-1} width. The frequency of ν_{NH} is red-shifted 108 cm^{-1} in going to S_1. This significant red-shift indicates that the NH bond weakens in S_1, suggesting that the molecule becomes a stronger acid in the excited state. Such an enhancement of acidity has also been reported in the photo-excitation of phenol and naphthol in aqueous solution.[35–42] The bandwidth is also

Table 1. Frequencies of the Observed ν_{NH} of Carbazole–$(H_2O)_1$ in S_0, and S_1

	ν_{NH}/cm^{-1}	bandwidth/cm^{-1}	$\delta^{a)}/cm^{-1}$
S_0	3426	< 5	
S_1	3318	< 10	108

a) Red shifts of the vibrational frequency from S_0 to S_1.

changed in S_1. The 5 cm^{-1} bandwidth in S_0 becomes two-times wider after electronic excitation to S_1. This broadening suggests that the relaxation process in S_1, especially in a higher vibronic level at ~3000 cm^{-1} region is accelerated significantly. This may be due to vibrational predissociation of the cluster. The mechanism of the photochemical reaction of carbazole will be discussed elsewhere along with all of the spectra, including other sized clusters, not only in S_1, but also in the cation state (D_0).

In conclusion, we constructed a picosecond IR-UV double-resonance spectrometer and demonstrated it by observations of the picosecond TRFD IR dip spectra of a phenol–$(H_2O)_1$ cluster in a supersonic jet. Our system with newly high-power mid-IR generation is enough to carry out IR dip spectroscopy. By employing both the counterpropagating setting and free jet expansion, we could obtain a frequency resolution of < 20 cm^{-1} and an instrument response time of approximately 25 ps.

Using this system, we measured the picosecond TRFD IR dip spectrum of a carbazole–$(H_2O)_1$ cluster. In TRFD IR dip spectroscopy, the spectral changes show clear vibrational structures of not only S_0, but also S_1 in the 2900–3800 cm^{-1} energy region. The frequencies of ν_{NH} of S_0 and S_1 were observed at 3426 and 3318 cm^{-1}, respectively, and were significantly red-shifted to 108 cm^{-1} in going from S_0 to S_1. This red-shift indicates that the NH bond weakens in S_1. The bandwidth is also significantly broadened in S_1, which suggests fast relaxation due to predissociation.

This picosecond time-resolved IR spectrometer can be applied not only to the spectroscopy of photo-excited molecules and clusters but also to the dynamics in which the time-evolution of specific intermediates must be measured. For example, we have successfully measured the picosecond time-resolved IR spectra of the transient species for the excited state hydrogen transfer of phenol–$(NH_3)_3$ cluster.[12] Moreover, in the ground state dynamics, we have measured the picosecond time-resolved IR spectra of 7-azaindole dimer for the intramolecular vibrational redistribution (IVR), and have revealed the mode-specific IVR dynamics in the picosecond time region.[43] These applications to the dynamics of aromatic molecules and clusters are now in progress.

The present work was financially supported in part by a Grant-in-Aid from the Ministry of Education, Science, Sports and Culture. Support from the Daiko Foundation is also gratefully acknowledged.

References

1 R. H. Page, Y. R. Shen, and Y. T. Lee, *J. Chem. Phys.*, **88**, 4621 (1988); *J. Chem. Phys.*, **88**, 5362 (1988).

2 T. S. Zwier, *Annu. Rev. Phys. Chem.*, **47**, 205 (1996).

3 T. Ebata, A. Fujii, and N. Mikami, *Int. Rev. Phys. Chem.*, **17**, 321 (1998).

4 B. Brutschy, *Chem, Rev.*, **100**, 3891 (2000).

5 E. G. Robertson and J. P. Simons, *Phys. Chem. Chem. Phys.*, **3**, 1 (2001).

6 C. Janzen, D. Spangenberg, W. Roth, and K. Kleinermanns, *J. Chem. Phys.*, **110**, 9898 (1999).

7 Th. Walther, H. Bitto, T. K. Minton, and J. R. Huber, *Chem. Phys. Lett.*, **231**, 64 (1994).

8 T. Ebata, N. Mizuochi, T. Watanabe, and N. Mikami, *J. Phys. Chem.*, **100**, 546 (1996).

9 E. G. Robertson, M. R. Hockridge, P. D. Jelfs, and J. P. Simons, *Phys. Chem. Chem. Phys.*, **3**, 786 (2001).

10 Y. Matsumoto, T. Ebata, and N. Mikami, *J. Phys. Chem. A*, **105**, 5727 (2001).

11 S. Ishiuchi, M. Saeki, M. Sakai, and M. Fujii, *Chem. Phys. Lett.*, **322**, 27 (2000).

12 S. Ishiuchi, M. Sakai, K. Daigoku, T. Ueda, T. Yamanaka, K. Hashimoto, and M. Fujii, *Chem. Phys. Lett.*, **347**, 87 (2001).

13 S. Lin and T. Suzuki, *Opt. Lett.*, **21**, 579 (1996).

14 D. E. Gragson, D. S. Alavi, and G. L. Richmond, *Opt. Lett.*, **20**, 1991 (1995).

15 G. M. Gale, G. Gallot, F. Hache, and R. Sander, *Opt. Lett.*, **22**, 1253 (1997).

16 P. Hamm, C. Lauterwasser, and W. Zinth, *Opt. Lett.*, **18**, 1943 (1993).

17 T. M. Jedju and L. Rothberg, *Appl. Opt.*, **27**, 615 (1988).

18 T. Fujino, M. Kashitani, K. Onda, A. Wada, K. Domen, C. Hirose, M. Ishida, F. Goto, and S. S. Kano, *J. Chem. Phys.*, **109**, 2460 (1998).

19 K. Domen, T. Fujino, A. Wada, and C. Hirose, S. S. Kano, *Appl. Surf. Scie.*, **121**, 484 (1997).

20 J. Aschenbrucker, M. Buback, N. P. Ernsting, J. Schroeder, and U. Steegmuller, *J. Phys. Chem. B*, **102**, 5552 (1998).

21 H. Okamoto and M. Tasumi, *Chem. Phys. Lett.*, **256**, 502 (1996).

22 G. Seifert, R. Zürl, T. Patzlaff, and H. Graener, *J. Chem. Phys.*, **112**, 6349 (2000).

23 G. Seifert, T. Patzlaff, and H. Graener, *Chem. Phys. Lett.*, **333**, 248 (2001).

24 M. A. F. H. van den Broek, H. -K. Nienhuys, and H. J. Bakker, *J. Chem. Phys.*, **114**, 3182 (2001).

25 A. J. Lock, S. Woutersen, and H. J. Bakker, *J. Phys. Chem. A*, **105**, 1238 (2001).

26 T. Ebata, M. Kayano, S. Sato, and N. Mikami, *J. Phys. Chem. A*, **105**, 8623 (2001).

27 J. C. Deak, L. K. Iwaki, and D. D. Dlott, *Opt. Lett.*, **22**, 1796 (1997).

28 J. C. Deak, L. K. Iwaki, S. T. Rhea, and D. D. Dlott, *J. Raman Spectrosc.*, **31**, 263 (2000).

29 D. D. Dlott, *Chem. Phys.*, **266**, 149 (2001).

30 S. Yamamoto, K. Kikuchi, and H. Kokubun, *Z. Phys. Chem.*, **109**, 47 (1978).

31 M. Martin, E. Breheret, F. Tfbel, and B. Lacourbas, *J. Phys. Chem.*, **84**, 70 (1980).

32 H. Masuhara, N. Tamai, N. Mataga, F. C. De Schryver, J. Vandendriessche, and N. Boens, *Chem. Phys. Lett.*, **95**, 471 (1983).

33 R. Bombach, E. Honegger, and S. Leutwyler, *Chem. Phys. Lett.*, **118**, 449 (1985).

34 M. Sakai, K. Daigoku, S. Ishiuchi, M. Saeki, K. Hashimoto, and M. Fujii, *J. Phys. Chem. A*, **105**, 8651 (2001).

35 T. Föster, *Z. Elektrochem.*, **54**, 531 (1950).

36 A. Weller, *Z. Physik. Chem.*, **17**, 224 (1958).

37 C. M. Harris and B. K. Sellnger, *J. Phys. Chem.*, **84**, 891 (1980).

38 C. M. Harris and B. K. Sellnger, *J. Phys. Chem.*, **84**, 1366 (1980).

39 D. Smith, N. G. Adams, and M. J. Henchman, *J. Chem. Phys.*, **72**, 4951 (1980).

40 S. P. Webb, L. A. Philips, S. W. Yeh, L. M. Tolbert, and J. H. Clark, *J. Phys. Chem.*, **90**, 5154 (1986).

41 R. Krshnan, T. G. Fillingim, J. Lee, and G. W. Robinson, *J. Am. Chem. Soc.*, **112**, 1353 (1990).

42 E. Pines and G. R. Fleming, *Chem. Phys.*, **183**, 393 (1994).

43 M. Sakai, S. Ishiuchi, and M. Fujii, *Eur. Phys. J. D*, **20**, 399 (2002).